Reac Kinet Mech Cat
DOI 10.1007/s11144-016-1102-x

Pd and In addition onto Au nanoparticles supported on TiO_2 as a catalytic formulation for NO_3^- reduction in water

Alejandra Devard[1] · Vanina S. Aghemo[1] · Carlos A. Caballero Dorantes[2] · Mirella Gutierrez Arzaluz[3] · F. Albana Marchesini[1] · María Alicia Ulla[1]

Received: 16 August 2016 / Accepted: 22 October 2016

Abstract The catalytic performance of Pd–In–Au/TiO_2 was studied for the reduction of nitrites and nitrates in water and compared with that of Au, Pd, Pd–In, In–Au and Pd–Au supported on TiO_2. Different characterization techniques were used to study the bulk and surface physicochemical properties of the trimetallic catalyst. The catalyst so obtained was active and stable in the nitrate reduction reaction, having a good selectivity to nitrogen. This improvement caused by the presence of gold is attributable to a strong interaction with surface palladium and can therefore act to regulate the hydrogenation activity of the Pd particles. Over 80% of Pd is deposited on top of the Au nanoparticles, which interact with surface Au during the reduction process. The NO_2^- species is an intermediate product in the NO_3^- reduction and the surface In–Pd intermetallic species are responsible for this first reaction step.

Keywords NO_3^- hydrogenation · Gold nanoparticles · Palladium · Indium · Titania

Introduction

Groundwater pollution due to industrial and agricultural activities has spread widely [1], representing a threat in numerous parts of the world, especially rural and suburban areas, in which groundwater is the only source of drinking water.

✉ María Alicia Ulla
mulla@fiq.unl.edu.ar

[1] Instituto de Investigaciones en Catálisis y Petroquímica - INCAPE (FIQ, UNL-CONICET), Santiago del Estero 2829, 3000 Santa Fe, Argentina

[2] Ciencia e Ingeniería Ambiental, Universidad Autónoma Metropolitana, Unidad Azcapotzalco, Mexico, D.F., Mexico

[3] Área de Química Aplicada, Departamento de Ciencias Básicas, Universidad Autónoma Metropolitana, Unidad Azcapotzalco, Mexico, D.F., Mexico

Published online: 01 November 2016

High concentrations of nitrates in drinking water are harmful due to their in situ reduction to nitrites (NO_2^-) [2], which may cause two adverse health effects, the induction of the "blue-baby syndrome" (methaemoglobinemia) especially in infants, and the potential formation of carcinogenic nitrosamines [3, 4]. Reverse osmosis, ion exchange and electrodialysis are processes to remove nitrates. However, these processes generate another environmental problem since they remove nitrates from raw water, but concentrate it in an effluent. On the other hand, there are promising methods that reduce nitrate to N_2, which is a harmless component. These methods are biological denitrification and heterogeneous catalytic systems [5, 6]. In the latter method, nitrates are reduced to N_2 by hydrogen in the presence of a bimetallic catalyst [7, 8]. Nevertheless, an over-reduction can take place generating ammonium as a side product, which is not desired in drinking water.

Bimetallic catalysts, which have been reported to be used in nitrate reduction in water, combine a noble metal such as Pd or Pt with another non noble metal like Cu, Sn, Ag or In, supported on oxides [9–18]. These noble/base metal combinations, usually based on Pd, show some promise in terms of nitrate removal rate [5] but they are usually limited in terms of the selectivity required to avoid undesired nitrite and ammonium formations [15]. Prusse et al. [18] reported that the improvement on nitrate reduction by the addition of In or Sn to the Pd supported on Al_2O_3 is higher than the one achieved by Cu incorporation. Besides, they demonstrated the efficiency of using formic acid as a reductant instead of hydrogen and the application of PVAL-encapsulated catalysts with superior diffusional properties.

Garron et al. [19] prepared catalysts for nitrate reduction adding Au to the Pd–Sn supported on SiO_2 and Al_2O_3. Trimetallic catalysts showed an increase in the conversion and selectivity to N_2. Moreover, the enhancement was more important on the Pd–Sn–Au/SiO_2 due to the formation of stable trimetallic particles.

Different oxides have been reported as good supports for the above mentioned bimetallic active components [15], among them Al_2O_3 [7, 9, 11, 12, 14], SiO_2 [7], ZrO_2 [10] and SnO_2 [10]. TiO_2 has also received considerable attention as a catalytic support due to its recognized photocatalytic activity and its contribution to the active sites [20–26]. In this vein, Kim et al. reported that the strong metal support interaction induced from the anatase-dominant TiO_2 support was crucial in promoting the activity of Pd-Cu/TiO_2 catalysts for nitrate reduction [27]. In addition, Soares et al., working with titanium dioxide, found that this material allowed a high activity to reduce nitrates; they also used a composite with carbon nanotubes, which significantly increased the selectivity to nitrogen in the process [15]. Krawczyk et al. [28] analyzed the influence of different supports on the selectivity to N_2. The prepared catalysts were Pd (5%), In (2%) supported on SiO_2, Al_2O_3 and TiO_2. These authors found that the most selective and stable catalyst was that supported on TiO_2. Moreover, it was demonstrated that the over-reduction of nitrate to ammonia depends on Pd-In interactions and also on the support porosity.

The aim of this work was to investigate a new catalytic formulation for nitrate reduction, where Au nanoparticles, Pd and In coexisted on a TiO_2 surface. Its activity and selectivity for the reduction of nitrites and nitrates were evaluated and compared with those of Au, In–Au and Pd–Au supported on TiO_2. In addition, the

physicochemical characterization of all the catalysts prepared was performed using different techniques to gain further insight into their active sites.

Experimental

Catalyst preparation

The support used was commercial TiO_2 (P25, DEGUSA) and four catalysts were produced: Au, In–Au, Pd–Au and Pd–In–Au supported on titania.

The primary catalyst, Au/TiO_2, was prepared via deposition–precipitation with NaOH and urea, according to the procedure reported by Zanella et al. [29]. Briefly, the titania powder (1 g) was dispersed in an aqueous solution of $HAuCl_4$ (Sigma Aldrich, p.a. 99.99%, 4.2×10^{-3} M, 100 mL), which corresponded to a theoretical Au loading of 8 wt%, in the case of a complete deposition. The solution temperature was fixed at 80 °C and the pH was adjusted around 8–9 with NaOH. After 1 h, the precursor solution was filtered. The solid so obtained was washed several times with distilled water and dried at 60 °C for 12 h. Next, it was treated in H_2 flow from 25 to 300 °C (heating rate: 5 °C min^{-1}) and kept at the final temperature for 2 h.

Indium was added to the Au/TiO_2 catalyst by wet impregnation using an In_2O_3 solution (Sigma Aldrich, p.a. 99.999%). The impregnation solution containing $InCl_3$ (aq) was prepared by the dissolution of In_2O_3 in HCl (aq). The amount of solution and concentration of indium was selected in order to obtain an In loading of 0.5 wt%. The catalyst reduction was performed in an atmosphere of H_2 to 450 °C during 1 h. The obtained catalyst was identified as $In–Au/TiO_2$.

The wet impregnation procedure was used to incorporate the palladium on the Au/TiO_2 catalyst. The impregnation solution containing $[PdCl_4]^{2-}$ was obtained by the dissolution of $PdCl_2$ in an acidic media (HCl 0.01 wt%). The amount of solution and concentration of palladium was selected in order to obtain 0.5 wt% Pd in the final catalyst ($Pd–Au/TiO_2$). After that, the catalyst was reduced in H_2 flow at 300 °C for 1 h (heating rate: 5 °C min^{-1}).

The latter procedure was also used to impregnate Pd on $In–Au/TiO_2$ to produce the ternary catalyst, $Pd–In–Au/TiO_2$. The reduction treatment was the same as that described for the Pd containing bimetallic catalyst.

Reaction experiments

Nitrite reduction

The reaction was performed under batch conditions, in a three-necked round bottom flask equipped with a magnetic stirrer (700–800 rpm) and a system for gas bubbling (H_2 4.8 or N_2 4.8). The pH value was controlled using an automatic pH controller unit. Experiments were carried out at room temperature and atmospheric pressure. The pH of 5 was maintained by adding HCl during the reaction test. All conditions were set in order to operate under chemical control.

Before the reaction, a volume of distilled water was loaded (80 mL) and purged with N_2 flow (200 cm^{-3} min^{-1}) for 20 min. Then, 200 mg of powder catalyst were added and the purge with N_2 was repeated under the same conditions as before. Finally, a H_2 flow of 400 cm^{-3} min^{-1} was bubbled for 20 min to saturate the solution and thus favor the catalyst surface reduction. Keeping the H_2 flow, the reaction started when a concentrated nitrite solution was added to the vessel in order to achieve 100 ppm of N-NO_2^- (concentration of nitrogen in the form of nitrite).

Nitrate reduction

After the reaction with nitrites, a concentrated nitrate solution was added to the vessel in order to obtain 50 or 100 ppm of N-NO_3^-.

The reaction progress was monitored by taking solution aliquots at different time intervals to determine the concentration of ammonium, nitrite and nitrate in the reaction medium. The nitrite chemical analysis was performed using the Griess method, the nitrate test was done using the reducing cadmium column followed of the Griess method [30] and the ammonium ion was analyzed by the modified Berthelot method. More details of the catalytic test of nitrate and nitrite reduction are given in [7].

The nitrate (NO_3^-) conversion was calculated according to Eq. 1.

$$X_{NO_3^-}\ (\%) = \left[\left(C^0_{NO_3^-} - C^t_{NO_3^-}\right)/C^0_{NO_3^-}\right] \times 100 \quad (1)$$

Here $C^0_{NO_3^-}$ is the initial N ppm of nitrate concentration, $C^t_{NO_3^-}$ is the N ppm of nitrate concentration at a given time.

Characterization

X-ray diffraction analysis (XRD)

The X-ray diffraction patterns of all the samples were obtained with a Shimadzu XD-D1 instrument, with Cu K_α radiation at 30 kV and 40 mA, scanning at 1° min^{-1} in the $2\theta = 10°$–$90°$ range. A Shimadzu XD-D1 analysis software package was used for phase identification.

Energy dispersive X-ray analysis (EDX)

Aliquots of the four prepared catalysts were covered using a system of carbon deposition, SPI SUPPLIES, 12157-AX, for EDX analysis. The samples were examined with a scanning electron microscope, JEOL, JSM 35C, equipped with an energy-dispersive X-ray analysis (EDX), which allowed the chemical elementary analysis. Semi-quantitative results were obtained by the theoretical quantitative method (SEMIQ), which does not require standards. The analytical methodology considered as 100% of all the elements detected and the percentage distribution were expressed on this basis.

X-ray photoelectron spectroscopy (XPS)

A multi-technique system (SPECS) equipped with a dual Mg/Al X-ray source and a hemispherical PHOIBOS 150 analyzer, operating in the fixed analyzer transmission (FAT) mode, was used to perform the X-ray photoelectron spectroscopy (XPS) analyses. The spectra were obtained with a pass energy of 30 eV and the Mg–K X-ray source was operated at 100 or 200 W. The working pressure in the analyzing chamber was less than 2×10^{-9} kPa. The XPS spectra of Pd 3d, Au 4d, Au 4f, In 3d, Ti 2p, O 1s, Cl 1s, K 2p and C 1s were recorded and all the binding energies were referenced to the surface Ti $2p_{3/2}$ peak at 459 eV. The data treatment was performed with the Casa XPS program (Casa Software Ltd., UK). The peak areas were determined by integration employing a Shirley-type background. For the quantification of the elements, sensitivity factors provided by the manufacturer were used.

Results and discussion

Catalytic NO_2^- reduction

Fig. 1 shows the NO_2^- and NH_4^+ concentration evolutions for nitrite reduction using Pd, Au, In–Au, Pd–Au, Pd–In–Au supported on TiO_2 as catalysts. The reaction evaluation for the Au/TiO_2 indicated that a conversion of 70% was achieved after 120 min, without NH_4^+ formation. Ammonium ion is an undesired by-product which is produced via a nitrite over-reduction. Thus, it is required that the catalyst should present a low selectivity to this by-product and thus favor the formation of nitrogen. The monometallic Pd/TiO_2 presented a conversion of 100% at 80 min, and a production of less than 10 ppm ammonium. When the In–Au/TiO_2 catalyst was tested for nitrite reduction during 120 min, the final conversion was 80% and NH_4^+ was not detected. The catalytic test of Pd–Au/TiO_2 after 30 min indicated that 100% conversion of nitrite was obtained with a 4 ppm N-NH_4^+ formation. Using Pd–In–Au/TiO_2 as catalyst, a 100% conversion and 9 ppm of N-NH_4^+ were obtained after a reaction time of 100 min.

Among the prepared catalysts (Fig. 1), the Pd containing samples (Pd/TiO_2, Pd–Au/TiO_2 and Pd–In–Au/TiO_2) were the most active catalysts for this reaction. Even though some NH_4^+ was produced, its final concentration was low compared with that of Pd alone [31–33]. These results suggested that the Au particles interacted with Pd, increasing the nitrite conversion and weakening the ammonium production. Mélendrez et al. [34] reported that the Pd particles with low coordination numbers (edges and corners) possessed high hydrogenation activity. They concluded that this type of active sites favored the nitrite over-reduction to ammonium, precisely because of their high hydrogenation activity.

Catalytic NO_3^- reduction

Sá et al. [35] demonstrated that 5 wt% Pd/TiO_2 was an active catalyst for the nitrate degradation process, where the titanium support could play an important role.

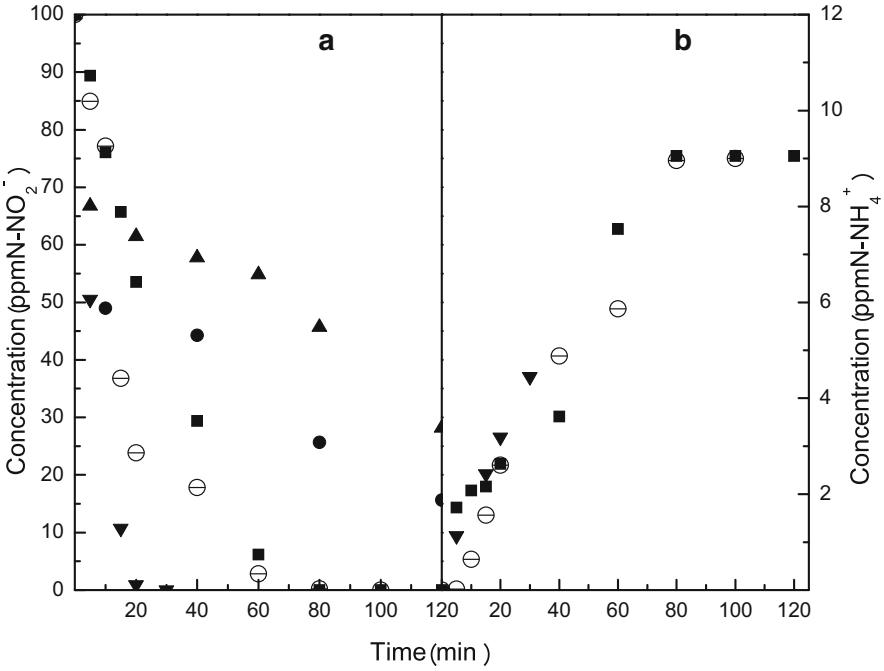

Fig. 1 Evolution of **a** NO_2^- concentration (ppm N-NO_2) and **b** NH_4^+ concentration as a function of reaction time in the presence of the (*filled triangle*) Au/TiO_2, (*filled square*) Pd/TiO_2, (*filled down-pointing triangle*) Pd–Au/TiO_2, (*filled circle*) In–Au/TiO_2, (*round circle with horizontal line*) Pd–In–Au/TiO_2 catalyst. *Reaction conditions* 100 ppm N-NO_2^-, catalyst = 200 mg/L, pH 5, F_{H_2} = 400 cm^3/min, T = 25 °C

However, that catalyst showed quite a low selectivity to N_2. On the other hand, Marchesini et al. [7] reported that the 1 wt% either Pd or Pt monometallic catalysts were not active for NO_3^- reduction using the same reaction conditions as applied in this work. Besides, it is well established in the open literature that the addition of a second metal (In [7, 16], Sn [10, 11, 26], Ag [12], Cu [12–15]) to the monometallic catalyst essentially generates active sites for the reduction from nitrate to nitrite (first reaction step), NO_2^- being an intermediate product [36]. The following reaction steps are the same as those of nitrite reduction.

The mono and bimetallic formulations, Pd//TiO_2, Au/TiO_2, In–Au/TiO_2 and Pd–Au/TiO_2, did not present any activity for nitrate reduction, suggesting that the In–Au and Pd–Au species so obtained were not capable of catalyzing the first reaction step, nitrate to nitrite. The catalytic performances of Pd–In/TiO_2 and Pd–In–Au/TiO_2 are presented in Fig. 2. The former catalyst reached a complete NO_3^- conversion in a short reaction time but with a high selectivity to NH_4^+ (NH_4^+ concentration: 81 ppm) [37]. Nevertheless, the Pd–In–Au/TiO_2 catalyst was active for nitrate reduction (70% conversion at 120 min) having an interesting low selectivity to ammonium (NH_4^+ concentration: 1.3 ppm). Therefore, the presence of Au in the tri-metallic catalyst (Pd–In–Au/TiO_2) promoted the NO_3^- reduction with a high selectivity to N_2.

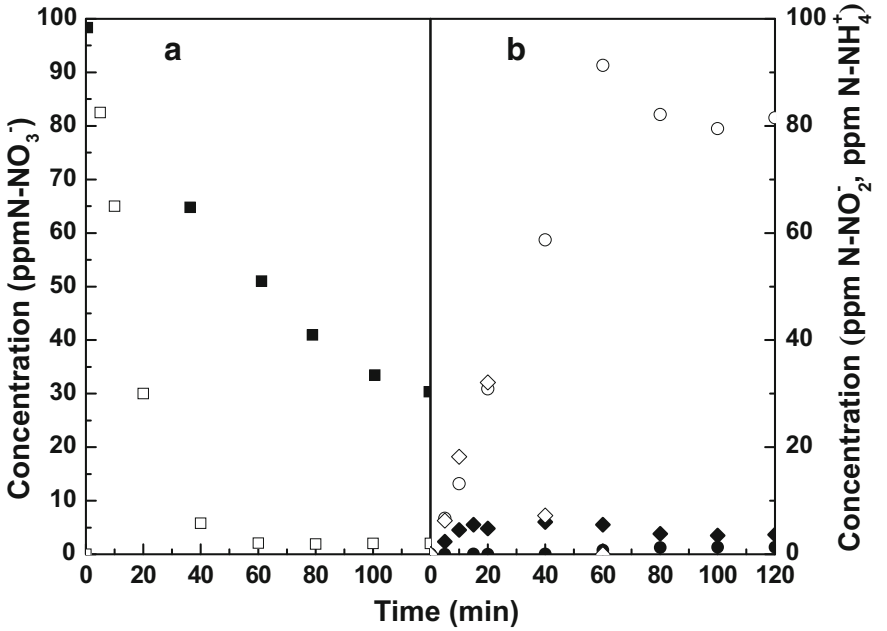

Fig. 2 Evolution of **a** NO_3^- (*filled square*, *open square*) concentration (ppm N-NO_3) and **b** NO_2^- (*filled diamond*, *open diamond*) and NH_4^+ (*filled circle*, *open circle*) concentrations as a function of reaction time in the presence of the Pd–In–Au/TiO_2 catalyst (*closed symbols*) and Pd–In/TiO_2 (*open symbols*). Reaction conditions: 100 ppm N-NO_3^-, catalyst = 200 mg/L, pH 5, F_{H_2} = 400 cm^3/min, T = 25 °C

Table 1 EDX analysis of the bulk metallic contents for the Pd–In–Au/TiO_2 catalyst

Catalyst	Bulk atomic ratio (10^2)			Weight percentage (wt%)		
	Au/Ti	Pd/Ti	In/Ti	Au	Pd	In
Fresh	4.36	0.57	0.53	5.84	0.44	0.44
Reduced	4.42	0.58	0.54	5.92	0.44	0.44

Catalyst bulk characterization

The Au, Pd and In weight percentages of the tri-metallic catalysts were determined through the EDX analysis. Table 1 shows the M/Ti ratio (M: Au, Pd or In) obtained for In–Pd–Au/TiO_2 as prepared (fresh catalyst) and after the reduction treatment in H_2 flow at 350 °C (reduced catalyst). The Au/Ti ratio was around 0.044 for the fresh and reduced samples and this value is consistent with the preparation method used [28]. The gold weight percentage estimated from this ratio is 5.8 wt%. The theoretical Pd and In loadings for the tri-metallic catalyst were close to those of the EDX detection limit, giving a ratio of Pd/Ti and In/Ti about 0.006. As the atomic weights of both elements are quite close, the calculated weight percentage of Pd and In are the same: 0.5 wt%.

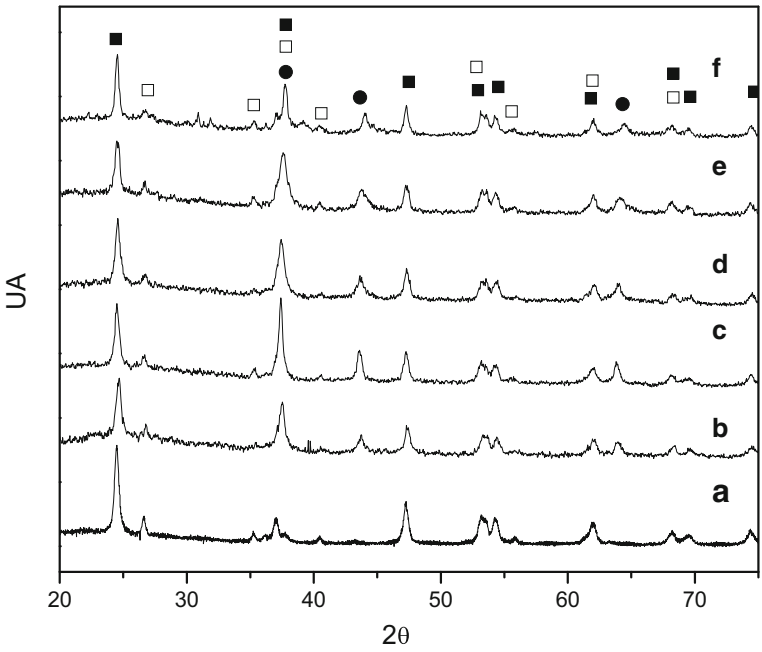

Fig. 3 X-ray diffraction patterns of *a* TiO_2, *b* Au/TiO_2, *c* In–Au/TiO_2, *d* fresh Pd–In–Au/TiO_2, *e* reduced Pd–In–Au/TiO_2, *f* used Pd–In–Au/TiO_2. *Symbols*: (*filled circle*) Au (4-784), (*filled square*) TiO_2 (21-1272), (*open square*) TiO_2 (21-1276)

The XRD pattern of the TiO_2 used as support is shown in Fig. 3a. The typical diffraction lines associated with the anatase structure were distinguished ($2\theta = 25°$, 37°, 48°, 53°, 55°, 62°, 71°, PDF 21-1272) with a small contribution of those of the rutile phase ($2\theta = 27°$, 36°, 39°, 41°, 44°, 54°, 56°, 64°, 68°, PDF 21-1276). According to Yuangpho et al. [38], the volume fraction of anatase and rutile phases can be estimated through the line intensity ratio between the anatase diffraction line at 25° and that of rutile at 27°; both lines are the most intensive ones for each structure. This ratio for the TiO_2 used in this work was 5.30; therefore, the anatase fraction was $x_{anatase} = 0.84$.

After the incorporation of gold onto the support, Au/TiO_2, the anatase/rutile ratio was 5.25 indicating that the $x_{anatase}$ was the same as that of the original support. This is an essential finding since Sá et al. [35] demonstrated that a TiO_2 having mainly anatase structure with a contribution of rutile could play an important role for the nitrite and nitrate ion reduction. Concerning the gold species, the metallic Au diffraction lines ($2\theta = 44.4°$ and 64.6°, PDF 4-784) were observed in the Au/TiO_2 XRD pattern (Fig. 3b). The average Au crystallite size was calculated using the Scherrer equation and this value was 24 nm.

The XRD patterns of In–Au/TiO_2 and Pd–In–Au/TiO_2 are shown in Figs. 3c and 3d, respectively. No significant differences are observed between these diffractograms and that of Au/TiO_2. Therefore, $x_{anatase}$ remained almost the same for all the prepared catalysts and the Pd and In species appeared to be well dispersed, avoiding

Table 2 Pd–In–Au/TiO_2

Catalyst	Ti $2p_{3/2}$	O 1s	Cl $2p_{3/2}$	K 2p	Pd $3d^a_{3/2}$	Au $4f^a_{7/2}$	In $3d_{5/2}$
Fresh	459.0	530.3	198.5	Nd	341.1 (83)	83.8 (90)	445.3
					342.8 (17)	85.6 (10)	
Reduced	459.0	530.2	198.6	Nd	340.3 (88)	83.5 (89)	445.1
					343.6 (12)	85.2 (11)	
Used	459.0	530.2	198.8	295.9	340.3 (69)	83.6 (90)	445.6
					343.6 (31)	85.3 (10)	

The binding energies of each element on its surface (eV)

[a] The contribution of each chemical state is between parentheses

the formation of large particles. However, the main diffraction lines of Pd and In species may overlap with those of TiO_2 (The main diffraction lines of InOx (PDF 6-416) are at $2\theta = 36.5°$ and 63.2°, for PdO at $2\theta = 54.8°$ and for $PdIn_3$ at $2\theta = 58.9°$ [34]). Moreover, Gao et al. [39] developed a promising catalyst for improving the catalytic reduction of nitrate, Pd–In/mesoporous alumina. According to the XRD results of this sample, the indium metallic particles have a characteristic peak at $2\theta = 54°$ while Pd^0 particles have characteristic peaks at $2\theta = 40°$ and 46°. Those peaks could also be masked with one of titania in the XRD patterns of Pd–In–Au/TiO_2.

Fig. 3d shows the diffractograms of Pd–In–Au/TiO_2 as prepared (fresh catalyst), after the reduction treatment and after being used under reaction conditions for 300 min. No significant differences were observed among the three XRD patterns, suggesting that the bulk phases remained stable after the different treatments.

Catalyst surface characterization

The chemical state of the different elements and their atomic ratio corresponding to the Pd–In–Au/TiO_2 surface were analyzed by XPS. The binding energies of K 2p, Ti 2p, O 1s, Cl 2p, Pd 3d, Au 4d, Au 4f and In 3d were determined. These measurements were carried out on the trimetallic catalyst so obtained, after its reduction with H_2 at 450 °C and after being used under reaction conditions for 120 min.

The XPS spectrum of Ti 2p for the fresh trimetallic catalyst presented the typical TiO_2 spectrum, corresponding to Ti $2p_{3/2}$ and Ti $2p_{1/2}$ in the Ti^{4+} oxidation state [40]. The BE of Ti $2p_{3/2}$ is shown in Table 2. No significant differences are observed comparing the spectrum described above with those of the reduced catalyst and the sample after being under reaction conditions (Table 2). Therefore, no reduction of surface Ti^{4+} took place.

The O 1s spectra for Pd–In–Au/TiO_2 under the three different conditions were asymmetrical, with a tail extending towards higher energies. The main signal of these three spectra was at 530.2 eV (Table 2) and assigned to the TiO_2 lattice oxygen. The extending tail was observed on the spectra of Au/TiO_2, TiO_2 anatase powder, anatase single crystal, nanocrystalline film among others and can be

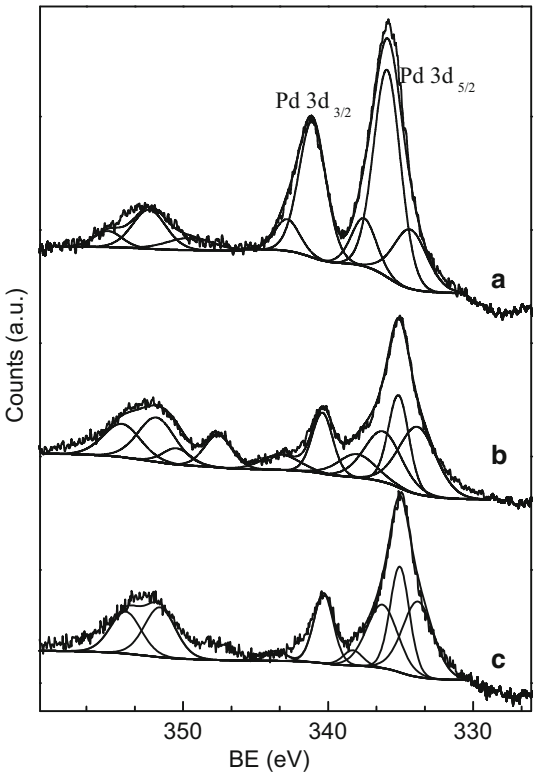

Fig. 4 XPS Pd 3d spectra of Pd–In–Au/TiO_2 and their fitted curves, *a* as prepared, *b* after being reduced with H_2 flow at 400 °C, *c* after being under reaction conditions for 120 min

attributed to surface hydroxyl groups and adsorbed water molecules [41]. The atomic ratios of O^{2-}/Ti^{4+} were 2.12 (a); 2.47 (b) and 2.06 (c); these ratios were slightly larger than the stoichiometric ratio: $O^{2-}/Ti^{4+} = 2.03$ in TiO_2 [41].

The presence of some residual chlorine from the metal salt precursor ($HAuCl_4$) was confirmed by the Cl 2p spectrum of the fresh sample (Table 2). After reduction, the surface Cl species decreased, as expected. However, a slight increment was observed in the Cl 2p spectrum of the used catalyst due to the addition of HCl during the catalytic evaluation in order to maintain a pH of 5.

The existence of K on the surface of the catalyst after being under reaction conditions was confirmed by the K 2p spectrum (Table 2). This result was a consequence of using KNO_3 as source of NO_3^- for the catalytic evaluation.

Fig. 4 shows the combined spectra of Au 4d and Pd 3d for the trimetallic catalyst, where the peak around 335.5 eV is the overlapping of Pd $3d_{5/2}$ and the Au $4d_{5/2}$ signals. Therefore, the Pd analysis was performed using the less intense Pd $3d_{3/2}$ signal. For the Au analysis, the Au $4f_{7/2}$ line was used.

The Pd $3d_{3/2}$ signal of the fresh sample was fitted with a main peak at 341.1 eV and a small one at 342.8 eV (Fig. 4a; Table 2). The 83% of surface Pd, which was associated with the peak at 341.1 eV, was in the form of metallic Pd^0 [42], whereas the component at high BE was associated with surface oxidized Pd species [43].

The Pd $3d_{3/2}$ spectrum obtained with the sample after being under reduction treatment showed the presence of two peaks with similar area ratios as observed in the previous spectrum (compare with Fig. 4). Nevertheless, the BEs were somehow different, 340.3 and 343.6 eV, suggesting changes in the chemical shifts in the surface Pd. Comparing the lower BE value of the reduced sample (340.3 eV) with that of the fresh one (341.1 eV), the negative shift of the former is evident, suggesting the formation of a Pd–Au alloy during the reduction treatment. A strong interaction between Au and Pd atoms can induce an electron transfer from Au to Pd, decreasing its BE as previously reported [44–46]. On the other hand, the BE of 343.6 eV was attributed to Pd^{2+} on PdO, indicating that some part of Pd (12%) remained without any interaction with surface Au. Even though these Pd atoms can be reduced during the treatment with H_2, they are easily re-oxidized in contact with air [47].

The BE values of Pd $3d_{3/2}$ for the Pd–In–Au/TiO_2 after being used under reaction conditions were 340.3 and 343.6 eV, indicating that the surface Pd species remained the same, Pd–Au Alloy and PdO. However, an increment in the amount of surface PdO was observed. This result was expected due to the fact that during the reaction, part of metallic Pd was oxidized producing the Pd^0/Pd^{2+} couple as active site [7, 48].

The In 3d spectra of the fresh and reduced catalysts indicated that the signal of In $3d_{5/2}$ was at 445.3 and 445.1 eV (Table 2). The BE around 445.5 eV is characteristic of In^{3+} (mainly In_2O_3) [49]. During the reduction treatment, the formation of some $In^{\delta+}$ was expected, which was validated by the shift to lower BE of the In $3d_{5/2}$ signal. The presence of $In^{\delta+}$ along with that of Pd^0 can generate surface intermetallic compounds. These surface bimetallic species are necessary to promote the first reaction step: the reduction from NO_3^- to NO_2^- [16, 39, 50].

The Au $4f_{7/2}$ peak of the fresh Pd–In–Au/TiO_2 involved two signals, one at 83.8 eV and another at 85.6 eV (Table 2; Fig. 5). The former, which is the main component, was associated with metallic gold and the latter, with oxidized Au species [51]. The Au 4f spectra of the trimetallic catalyst after being in reduction treatment and under reaction conditions were quite similar to those described above. Nevertheless, a small BE shift of Au^0 was visible (Table 2), which could be attributed to a Pd–Au interaction and a surface alloy formation [52].

Distribution of surface Pd, In and Au active sites

The surface Pd/Au and In/Au ratios of the fresh catalyst were close to 1 (Table 3) although these atomic ratios referred to the bulk were 0.125 (Table 1), indicating surface enrichment of Pd and In against Au. Even though these surface ratios decreased after being under reaction conditions (Table 3), the values so obtained were larger than those of bulk atomic ratios.

Considering the XPS analysis for Pd, In and Au and their surface distributions, it is possible to figure out how these species are on the TiO_2 surface (Fig. 6):

(i) Part of Pd is deposited on top the Au nanoparticles and during the reduction process the surface Pd–Au alloy is developed by decreasing the BEs of both components.

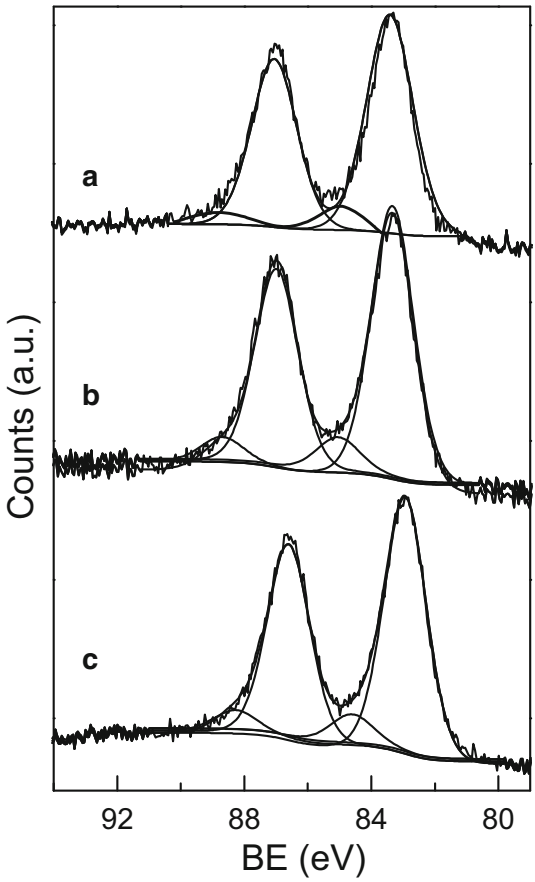

Fig. 5 XPS Au 4f spectra of Pd–In–Au/TiO_2 and their fitted curves, *a* as prepared, *b* after being reduced with H_2 flow at 400 °C, *c* after being under reaction conditions for 120 min

Table 3 The surface atomic ratio of the active components on Pd–In–Au/TiO_2

Catalyst	(Pd/Au)s	(In/Au)s	(Pd/In)s
Fresh	1.10	1.06	1.04
Reduced	0.38	0.09	3.84
Used	0.36	0.23	1.62

(ii) The rest of Pd remains on the TiO_2 surface as Pd^{2+}. Even if these particles are reduced in H_2 at 400 °C, they can be reoxidized in contact with air [48].

(iii) The In onto the titania is mainly as In_2O_3. However, during the reduction treatment, some surface In–Pd intermetallic species can be produced.

Therefore, surface In–Pd intermetallic species act as active sites in the first reaction step of the nitrate reduction in water, producing NO_2^-, which is then reduced mainly to N_2 through the Pd–Au alloy and PdO_x.

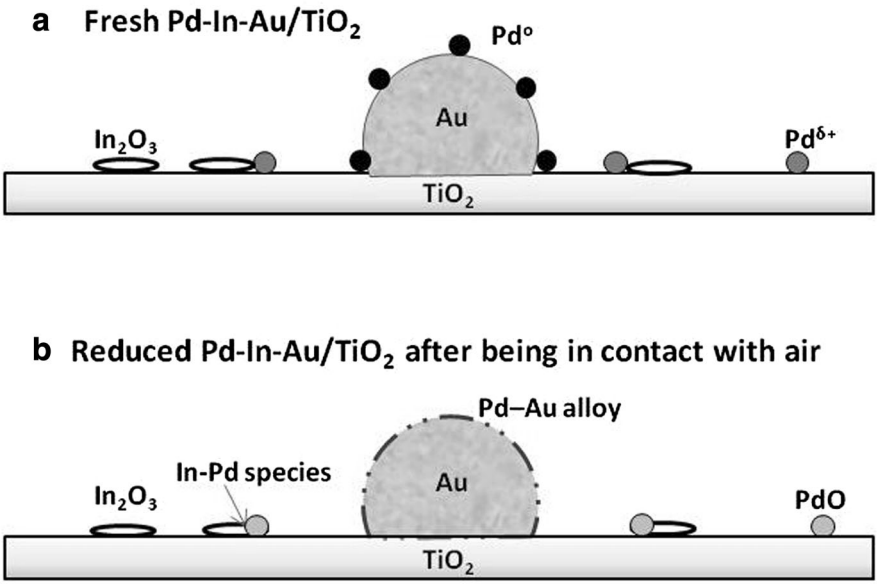

Fig. 6 Scheme of surface species on the Pd–In–Au/TiO_2: **a** as prepared and **b** after the reduction treatment with H_2 flow at 400 °C

Conclusions

The addition of Pd and In to the gold nanoparticles supported onto TiO_2 generated a trimetallic catalyst with good activity for nitrate reduction in water, limiting the over-reduction to NH_4^+.

The improvement caused by the presence of gold is attributable to a strong interaction with surface palladium and can therefore act to regulate the hydrogenation activity of Pd particles.

More than 80% of Pd is deposited on top of the Au nanoparticles, which interact with surface Au during the reduction process, thus developing a surface Pd–Au alloy. The rest of Pd is present on the titania surface as oxidized Pd species. The presence of the Pd^0/Pd^{2+} couple plays an important role as active site for the NO_2^- reduction.

The NO_2^- species is an intermediate product on the NO_3^- reduction and the surface In–Pd intermetallic species are responsible for this first reaction step.

Acknowledgements The authors acknowledge the financial support received from ANPCyT, UNL and CONICET. They are also grateful to ANPCyT for the purchase of the SPECS multitechnique analysis instrument (PME8-2003). Thanks are also given to Fernanda Mori for the XPS measurements. CACD thanks Universidad Autónoma Metropolitana (Mexico) for funding his stay at INCAPE (Argentina).

References

1. Bhatnagar A, Sillanpää M (2011) A review of emerging adsorbents for nitrate removal from water. Chem Eng J 168:493–504
2. Canter LW (1997) Nitrates in groundwater. CRC Press, Boca Raton
3. Yang C-Y, Wu D-C, Chang C-C (2007) Nitrate in drinking water and risk of death from colon cancer in Taiwan. Environ Int 33:649–653
4. Tate CH, Arnold KF (1990) Health and aesthetic aspects of water quality. In: Pontius FW (ed) Water Quality and Treatment. McGraw-Hill Inc., New York, pp 63–156
5. Barrabés N, Sá J (2011) Catalytic nitrate removal from water, past, present and future perspectives. Appl Catal B: Environ 104:1–5
6. Aritizábal A, Barrabés N, Contreras S, Kolafa M, Tichit D, Medina F, Sueiras J (2010) Pt/CuZnAl mixed oxides for the catalytic reduction of nitrates in water: study of the incidence of the Cu/Zn atomic ratio. Phys Procedia 8:44–48
7. Marchesini FA, Irusta S, Querini C, Miró E (2008) Nitrate hydrogenation over Pt, In/Al_2O_3 and Pt, In/SiO_2. Effect of aqueous media and catalyst surface properties upon the catalytic activity. Catal Commun 9:1021–1026
8. Aristizábal A, Kolafa M, Contreras S, Domínguez M, Llorca J, Barrabés N, Tichit D, Medina F (2011) Catalytic activity and characterization of Pt/calcined CuZnAl hydrotalcites in nitrate reduction reaction in water. Catal Today 175:370–379
9. Prüsse U, Hälhein M, Daum J, Vorlop KD (2000) Improving the catalytic nitrate reduction. Catal Today 55:79–90
10. Gavagnin R, Biasetto L, Pinna F, Strukul G (2002) Nitrate removal in drinking waters: the effect of tin oxides in the catalytic hydrogenation of nitrate by Pd/SnO_2 catalysts. Appl Catal B 38:91–99
11. Berndt H, Mönnich I, Lücke B, Menzel M (2001) Tin promoted palladium catalysts for nitrate removal from drinking water. Appl Catal B 30:111–122
12. Gauthard F, Epron F, Barbier J (2003) Palladium and platinum-based catalysts in the catalytic reduction of nitrate in water: effect of copper, silver, or gold addition. J Catal 220:182–191
13. Barrabes N, Just J, Dafinov A, Medina F, Fierro JLG, Sueiras JE, Salagre P, Cesteros Y (2006) Catalytic reduction of nitrate on Pt–Cu and Pd–Cu on active carbon using continuous reactor: the effect of copper nanoparticles. Appl Catal B 62(1–2):77–85
14. Palomares AE, Franch C, Corma A (2010) Nitrates removal from polluted aquifers using (Sn or Cu)/Pd catalysts in a continuous reactor. Catal Today 149:348–351
15. Soares OSGP, Órfão JJM, Pereira MFR (2011) Nitrate reduction in water catalysed by Pd–Cu on different supports. Desalination 279:367–374
16. Pizarro AH, Molina CB, Rodriguez JJ, Epron F (2015) Catalytic reduction of nitrate and nitrite with mono- and bimetallic catalysts supported on pillared clays. J Environ Chem Eng 3:2777–2785
17. Strukul G, Gavagnin R, Pinna F, Modaferri E, Perathoner S, Centi G, Marella M, Tomaselli M (2000) Use of palladium based catalysts in the hydrogenation of nitrates in drinking water: from powders to membrane. Catal Today 55:139–149
18. Prusse U, Hahnlein M, Daum J, Vorlop K-D (2000) Improving the catalytic nitrate reduction. Catal Today 55:79–90
19. Garron A, Lázár K, Epron F (2006) Characterization by Mössbauer spectroscopy of trimetallic Pd–Sn–Au/Al_2O_3 and Pd–Sn–Au/SiO_2 catalysts for denitration of drinking water. Appl Catal B 65:240–248
20. Anderson JA (2012) Simultaneous photocatalytic degradation of nitrate and oxalic acid over gold promoted titania. Catal Today 181:171–176
21. Jin R, Gao W, Chen J, Zeng H, Zhang F, Liu Z, Guan N (2004) Photocatalytic reduction of nitrate ion in drinking water by using metal-loaded $MgTiO_3$–TiO_2 composite semiconductor catalyst. J Photochem Photobiol A: Chem 162:585–590
22. Zhang F, Jin R, Chen J, Shao C, Gao W, Li L, Guan N (2005) High photocatalytic activity and selectivity for nitrogen in nitrate reduction on Ag/TiO_2 catalyst with fine silver clusters. J Catal 232:424–431
23. Li Y, Wasgestian F (1998) Photocatalytic reduction of nitrate ions on TiO_2 by oxalic acid. J Photochem Photobiol A: Chem 112:255–259

24. Kominami H, Nakaseko T, Shimada Y, Furusho A, Inoue H, Murakami S, Kera Y, Ohtani B (2005) Selective photocatalytic reduction of nitrate to nitrogen molecules in an aqueous suspension of metal-loaded titanium(IV) oxide particles. Chem Commun 23:2933–2935
25. Ranjit KT, Varadarajan TK, Viswanathan B (1995) Photocatalytic reduction of nitrite and nitrate ions to ammonia on Ru/TiO_2 catalysts. J Photochem Photobiol A: Chem 89:67–68
26. Ranjit KT, Viswanathan B (1997) Photocatalytic reduction of nitrite and nitrate ions over doped TiO_2 catalysts. J Photochem Photobiol A: Chem 107:215–220
27. Kim M-S, Chung S-H, Yoo C-J, Lee MS, Cho I-H, Lee D-W, Lee K-Y (2013) Catalytic reduction of nitrate in water over $Pd–Cu/TiO_2$ catalyst: effect of the strong metal-support interaction (SMSI) on the catalytic activity. Appl Catal B 142–143:354–361
28. Krawczyk N, Karski S, Witonska I (2011) The effect of support porosity on the selectivity of Pd–In/support catalysts in nitrate reduction. Reac Kinet Mech Cat 103:311–323
29. Zanella R, Delannoy L, Louis C (2005) Mechanism of deposition of gold precursors onto TiO_2 during the preparation by cation adsorption and deposition–precipitation with NaOH and urea. Appl Catal A: Gen 291:62–72
30. APHA (1992) Standard methods for the examination of water and wastewater, 21st edn. APHA, Washington
31. Lee J, Gul Hur Y, Kim M-S, Lee K-Y (2015) Catalytic reduction of nitrite in water over ceria- and ceria–zirconia-supported Pd catalysts. J Mol Catal A: Chem 399:48–52
32. Chinthaginjala JK, Villa A, Su DS, Mojet BL, Lefferts L (2012) Nitrite reduction over Pd supported CNFs: metal particle size effect on selectivity. Catal Today 183:119–123
33. Yoshinaga Y, Akita T, Mikami I, Okuhara T (2002) Hydrogenation of nitrate in water to nitrogen over Pd–Cu supported on active carbon. J Catal 207:37–45
34. Mélendrez R, Del Angel G, Bertin V, Valenzuela MA, Barbier J (2000) Selective hydrogenation of carvone and o-xylene on Pd–Cu catalysts prepared by surface redox reaction. J Mol Catal A 157:143–149
35. Sá J, Berger T, Föttinger K, Riss A, Anderson JA, Vinek H (2005) Can TiO_2 promote the reduction of nitrates in water? J Catal 234:282–291
36. Especel C, Duprez D, Epron F (2014) Bimetallic catalysts for hydrogenation in liquid phase. C R Chim 17:790–800
37. Marchesini FA (2008) Doctoral Thesis, Universidad Nacional del Litoral, Argentina
38. Yuangpho N, Le STT, Treerujiraphapong T, Khanitchaidecha W, Nakaruk A (2015) Enhanced photocatalytic performance of TiO_2 particles via effect of anatase–rutile ratio. Physica E 67:18–22
39. Gao Z, Zhang Y, Li D, Werth C, Zhang Y, Zhou X (2015) Highly active Pd–In/mesoporous alumina catalyst for nitrate reduction. J Hazard Mater 286:425–431
40. Wang Y, Zhong M, Chen F, Yang J (2009) Visible light photocatalytic activity of TiO_2/D-PVA for MO degradation. Appl Catal B 90:249–254
41. Kruse N, Chenakin S (2011) XPS characterization of Au/TiO_2 catalysts: binding energy assessment and irradiation effects. Appl Catal A 391(1–2):367–376
42. Venezia A, La Parola V, Pawelec B, Fierro JLG (2007) Hydrogenation of aromatics over $Au–Pd/SiO_2–Al_2O_3$ catalysts; support acidity effect. Appl Catal A 264:43–51
43. Kalevaru NN, Benhmid A, Radnik J, Pohl M, Bentrup U, Martin A (2007) Marked influence of support on the catalytic performance of PdSb acetoxylation catalysts: effects of Pd particle size, valence states, and acidity characteristics. J Catal 246:399–412
44. Shi Y, Zhao X, Cao T, Chen J, Zhu W, Yu Y, Hou Z (2012) Au–Pd nanoparticles on layered double hydroxide: highly active catalyst for aerobic oxidation of alcohols in aqueous phase. Catal Commun 18:142–146
45. Suo Z, Ma C, Jin M, He T, An L (2008) The active phase of $Au–Pd/Al_2O_3$ for CO oxidation. Catal Commun 9:2187–2190
46. Wang H, Wang C, Yan H, Yi H, Lu J (2015) Precisely-controlled synthesis of Au–Pd core–shell bimetallic catalyst via atomic layer deposition for selective oxidation of benzyl alcohol. J Catal 324:59–68
47. Herzing A, Carley AF, Edwards JK, Hutchings GJ, Kiely CJ (2008) microstructural development and catalytic performance of Au–Pd nanoparticles on Al_2O_3 supports: the effect of heat treatment temperature and atmosphere. Chem Mater 20:1492–1501
48. Devard A, Ulla MA, Marchesini FA (2013) Synthesis of Pd/Al_2O_3 coating onto a cordierite monolith and its application to nitrite reduction in water. Catal Commun 34:26–29

49. Yang X, Wang Y, Xu L, Yu X, Guo Y (2008) Silver and indium oxide codoped TiO_2 nanocomposites with enhanced photocatalytic activity. J Phys Chem C 112:11481–11489
50. Witonska I, Karski S, Rogowski J, Krawczyk N (2008) The influence of interaction between palladium and indium on the activity of Pd–In/Al_2O_3 catalysts in reduction of nitrates and nitrites. J Mol Catal A: Chem 287(1–2):87–94
51. Sterchele S, Biasi P, Centomo P, Campestrini S, Shchukarev A, Rautio A-R, Mikkola J-P, Salmi T, Zecca M (2015) The effect of the metal precursor-reduction with hydrogen on a library of bimetallic Pd–Au and Pd–Pt catalysts for the direct synthesis of H_2O_2. Catal Today 248:40–47
52. Kittisakmontree P, Yoshida H, Fujita S, Arai M, Panpranot J (2015) The effect of TiO_2 particle size on the characteristics of Au–Pd/TiO_2 catalysts. Catal Commun 58:70–75